Manuscript MR-D-17-00926 -Revised

Evaluation of Screen Printed Silver Trace Performance and Long-Term Reliability against Environmental Stress on a Low Surface Energy Substrate

Riikka Mikkonen, Matti Mäntysalo*

M. Sc. R. Mikkonen, Prof. M. Mäntysalo

Tampere University of Technology, Laboratory of Electronics and Communications Engineering,

Korkeakoulunkatu 3, 33720 Tampere, Finland

*Contact details: riikka.mikkonen@tut.fi, +358504481269.

Abstract

Otherwise attractive substrate materials for printed electronics may have such surface characteristics that make patterning challenging. This article focuses on the printability and performance characterization of conductive patterns on a low surface energy substrate. Surface characteristics of a hydrophobic polyphenylene ether (PPE) substrate and the effects of surface modification using chemical and physical pre-treatments were studied. In addition, silver ink performance and its reliability on this substrate were evaluated. The surface was characterized by surface energy measurements and surface profile analysis. Screen-printed test patterns were characterized to evaluate print quality and electrical and mechanical performance. A further inspection of substrate-ink interactions was conducted using environmental reliability tests. It was observed that ink adhesion could be significantly promoted by choosing a suitable surface pre-treatment method. Low sheet resistances were obtained, and thus, suitable inks for further characterization were found. In addition, it was observed that environmental stress has a significant impact on ink-substrate interactions.

Keywords: Printed electronics, PPE, surface modification, adhesion, environmental stress, reliability

1. Introduction

Printed electronics (PE) make it possible to fabricate intelligent applications with the potential to revolutionize the future electronics market. The importance of printed electronics is emphasized in various sensing and monitoring applications, where thin and wireless devices on flexible and stretchable platforms enable device integration into an everyday environment, and are thus one of the key applications on the path towards the Internet of Everything (IoE) [1–6].

Since many sensing applications operate at high frequencies, it is necessary to find materials enabling sufficient functionality in this area. Proper functionality of printed high frequency (HF) structures places requirements on both the coating and substrate materials. For example, conductive material should be selected so that DC sheet resistance is as low as possible. In addition, printed conductors should be smooth to enable fast signal transmission. On the other hand, basic substrate requirements include low relative permittivity and dissipation factor to prevent signal attenuation via the substrate material [1,7,8].

Furthermore, materials should be selected so that ink-substrate interface interactions enable proper wetting of the substrate and sufficient ink adhesion on the used substrate material. These properties may be enhanced by, for example, surface modification prior to printing. Thus, the substrate surface is altered by modifying the chemical compound and surface profile [9,10]. In addition to the initial performance characterization of the printed structures, a reliability study is necessary in the development of printed electronics. For example, relatively thin and soft printed lines can easily be scratched. Additionally, structures have to endure plenty of stress during product lifetime. By using accelerated reliability tests, the long-term reliability of the applications may be inspected efficiently, without the need to wait until the end of product lifetime during normal usage [11]. With these tests, such material interfaces can be found that make printed structures better able to endure environmental stress and remain reliable, even in harsh environments [12].

In this study, the authors continue their earlier benchmark study of silver ink performance on a PPE-based HF substrate material [13]. This polymer compound is designed for GHz applications, with a dissipation factor below 0.001 and a dielectric constant of 2.60 [14]. Therefore, it is an attractive substrate material for

applications operating in the GHz range and could be used as a platform for printed large-area antennas and other wireless applications, such as molded interconnect devices. The variety of studied silver inks has been broadened and the effects of new surface pre-treatments on substrate material are studied. Environmental stress tests (85 % relative humidity (RH) /85 °C test, cyclic salt mist test) are used to evaluate the effect of elevated temperature and salt exposure in humid conditions on long-term reliability.

2. Experimental section

Figure 1 introduces the reader to the process steps and test variables included in this survey. A detailed

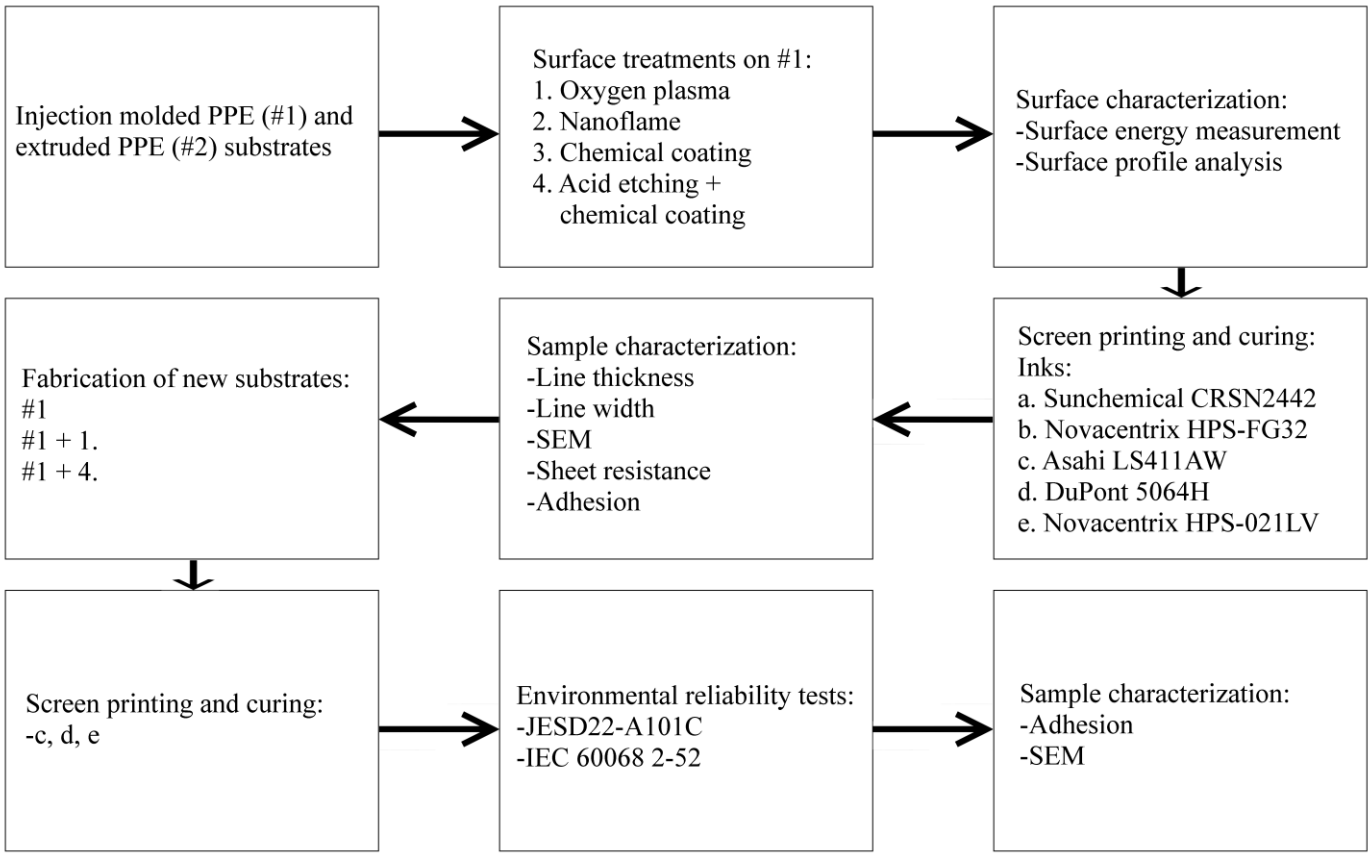

discussion of both materials and methods is included in the following sections.

Figure 1. Test matrix including all variables and process steps.

2.1. Materials

The purpose of this study was to continue the authors' benchmark study of silver ink printability on PPE, and therefore, an injection-molded PPE substrate (10 cm x 10 cm) with 3 mm thickness was used. In addition, an extruded PPE substrate (10 cm x 10 cm) with 1 mm thickness was studied to compare the effects of the molding process and substrate thickness on the surface parameters and final performance. These substrates are relatively thick for convenctional printed electronics applications. However, since our purpose is to find HF applicable materials, which are suitable for fabrication of three-dimensional (3D) objects, like molded interconnect devices, or large area devices, substrate dimensions are considered sufficient for our purposes.

In our earlier study [13], SunChemical CRSN2442 and DuPont 5064H screen printing inks were used. Since low sheet resistances were obtained, research was continued to inspect the effects of substrate surface pre-treatments further. In addition, three other silver inks were selected for further comparison of the conductive materials. The most critical ink parameters obtained from the datasheets are listed in table 1.

All of the selected inks have high silver contents, which helps decrease the sheet resistance of the printed structures. In addition, inks with different viscosities were selected to inspect their effect on print quality, and thus, on conductor performance. Furthermore, inks with different solvents were selected to compare their properties. HPS-021LV differs from other inks because it is aqueous. This aqueous ink is more environmentally friendly than other inks, and is therefore an attractive choice. In the extant literature, this ink has been studied, for example, in works by Sipilä [15] and Björninen [16], where it was successfully used to print HF structures on challenging substrates, such as plywood and textiles.

Other studies on the selected inks include, for example, a work by Happonen [17], where 5064H was compared to LS411AW via sheet resistance and bending abilities. The results indicated that excellent electrical performance could be obtained with both inks, but they were not successful with the cyclic bending tests. LS411AW was also included in studies by Jansson [18] and Voutilainen [19], where it was

used to fabricate more complex structures, such as moisture sensors [18] as well as inductors and capacitors [19]. The results indicated that low sheet resistances could be obtained and that the structures can endure environmental stress well.

Table 1. Material parameters of the used conductive inks [20-24].

Ink Manufacturer	Ag [%]	Solvent	Viscosity [cP]	Sheet resistance [$m\Omega\square^{-1}$@thickness]
CRSN2442 SunChemical	69–71	propylene diacetate	2000–3000	10@25µm
5064H DuPont	63–66	C11-ketone	10,000–20,000	<14@25µm
LS411AW Asahi	65–75	butyl cellosolve acetate, isophorone	20,000–30,000	<40@10µm
HPS-FG32 Novacentrix	75	butyl carbitol	8000	25@25µm
HPS-021LV Novacentrix	75	water	2600	≤14@25µm

2.2. Methods

2.2.1. Surface pre-treatment methods

The authors observed previously that oxygen plasma treatment is a sufficient surface treatment for enhancing the adhesion of a substrate-ink interface [13]. Therefore, it was used in this survey to see if it would also work with other inks. However, etching with sulfuric acid (H_2SO_4) or potassium hydroxide (KOH) did not improve the performance results.

Since sulfuric acid had an increasing effect on the substrate surface energy, though, it was nevertheless used in this survey as a base for chemical coating with ethyltriglycol. To inspect the effect of prior acid etching on coating behavior, ethyltriglycol was also applied to the native PPE. Since the native PPE was not wetted as well as the pretreated substrate, three layers of coating were applied. All coated samples were

cured in an oven at 100 °C for 15 minutes after each coating layer had been applied. A summary of the chemical treatment parameters that were used is provided in table 2.

Table 2. Chemical coating parameters.

Substrate	Coating layers	Curing conditions
Native PPE	3	100 °C/15 min
PPE with 5min. H_2SO_4 etching	1	100 °C/15 min

In addition, physical flame-pyrolytic silicating via a Nanoflame pistol [25] was used. With this technique, surface is modified via formation of silicon dioxide layer on the treated surface. This surface treatment has been used successfully in prior studies to modify substrates and as an adhesion promoter, for example in a study by Pekkanen [26]. A Polytec Nanoflame pistol was used to heat the substrate surface and, at the same time, the heated pistol gas formed silica oxides on the substrate surface. Due to the large surface area and rapid heating of the substrate, substrates were first treated from one direction, after which the substrate was rotated 90° and the treatment was repeated to ensure an even treating of surface. The extruded, 1 mm thick PPE substrate was used without any additional surface pre-treatment.

2.2.2. Screen printing and post-treatment

When all substrates had been prepared, test patterns were printed in cleanroom conditions with a semimanual single sheet screen printer SCF300. An aluminum screen with NBC UX79-45 polyester mesh (opening 81 µm, theoretical wet thickness 27.7 µm) [27] was used. After printing, the samples were cured in an oven according to datasheet recommendations: HPS-021LV was cured at 150 °C for 30 minutes, HPS-FG32 at 140 °C for 10 minutes, CRSN2442 at 150 °C for 30 minutes, LS411AW at 150 °C for 20 minutes, and 5064H at 130 °C for 20 minutes.

2.3. Environmental reliability tests

In addition to the initial performance evaluation, accelerated reliability tests were executed to assess the effects of environmental stress on mechanical performance. First, a JEDEC JESD22-A101C 500 h storage test (85 °C temperature and 85 % relative humidity (RH)) was used [28]. This test is widely used to evaluate product aging in normal storing conditions. Samples were placed into a Weiss C340 chamber.

In addition, an IEC 60068 2-52 salt mist test was used to inspect the aging effect of high relative humidity in a salty environment [29]. This test is important for structures aimed at outdoor applications and especially in a marine environment. For this test, the samples were first exposed to sodium chloride (NaCl) mist for two hours, after which time they were kept in 93 % RH for 168 h. This cycle was then repeated. The samples were placed in an Ascott S450XP chamber during this test. To minimize the effect of uneven salt spray in the chamber, the samples were placed in random order into the chamber. After the test, the samples were rinsed with deionized (DI) water to remove the excess salt and, thus, to suspend any corrosive reactions.

2.4. Characterization

For comparison of the surface pre-treatment effects, an optical profilometer Veeco Wyko NT1100 was used to measure the surface profiles of the fabricated substrates. Roughness data was collected from the measured profile range R_t. Range is determined as the difference between the highest peak and lowest valley of the surface profile as follows:

$$R_t = R_p - R_v, \tag{1}$$

where R_p is the highest peak and R_v is the lowest valley of the substrate. In addition, RMS roughness R_q was used for roughness data collection. R_q is calculated as follows:

$$R_q = \frac{1}{n}\sum_{i=1}^{n} y_i^2, \tag{2}$$

where y is the deviation over the roughness mean and n is the number of samples [30]. Since this parameter is greatly affected by deviations from the surface mean line, it is a good data parameter for rough surfaces.

In addition, a set of Dyne pens with a surface tension range of 30 – 60 mNm^{-1} were used to measure the surface energies of all substrates. With this method, surface energy is determined by drawing a line on the substrate with a test pen. Ink either forms a continuous line on the surface or withdraws back into droplets, depending on the surface tension of the ink.

Printed line thicknesses were measured with an optical profilometer using the roughness parameters R_t and R_q. A scanning electron microscope (SEM) was used to inspect the surface topology of the cured ink structures. In addition, an optical microscope was used to measure the conductor line widths.

The electrical performance of the printed samples was evaluated using a four-point probe (4PP) sheet resistance measurement and a crosscut adhesion test. First, supply current I (10mA) was fed to the printed conductor pattern and the resulting voltage difference U was measured with a Keithley 2425 sourcemeter. The obtained values and conductor dimensions (width w = 1.3 mm, length l = 32 mm) were then used to calculate sheet resistance R_s:

$$R_s = \frac{U}{I}\frac{w}{l}. \qquad (3)$$

The electrical performance of the samples was not measured after the reliability tests, since prior studies by, for example, Caglar [31], Halonen [32] and Xie [2] have stated that the sheet resistance of silver conductors is not altered significantly in similar environmental stress tests, in comparison to the drastic adhesion degradation that was reported after these tests. Therefore, only interface adhesion was evaluated here, and electrical performance characterization was left to further stages of research, where possible effects on, for example, HF performance will be studied.

Additionally, a square pattern (2 cm x 2 cm) was used to evaluate the initial mechanical performance of the substrate-ink interface after curing and to inspect the effects of environmental stress. For this evaluation, a crosscut adhesion test was executed according to the ASTM-D3359 standard [33]. This standard is widely used for adhesion rating in the field of printed electronics, and it was therefore considered a suitable test method for this study [34–38].

3. Results

3.1. Substrate surface characteristics

3.1.1. Surface energy

Table 3 shows the measured surface energies for each test substrate type. The surface energies of the extruded PPE and injection-molded PPE matched due to the similar chemical compound. We observed that original surface energy value of the PPE substrate could be at least doubled with oxygen plasma and Nanoflame surface treatments. These results suggest that new functional groups were formed on substrate surface. On the other hand, ethyltriglycol coating sprayed on the native PPE did increase the surface energy partially. This result was mainly due to the uneven wetting of the chemical-substrate interface. We observed that ethyltriglycol could not wet native PPE even when multiple coating layers were applied, whereas the acid-etched substrate was wetted extremely well even with one coating layer. We had observed earlier in [13] that etching with sulfuric acid increased the surface energy of PPE significantly (56–58 mN/m). Therefore, it is likely that ethyltriglycol wetting is improved on acid-etched substrate, because chemical surface tension and substrate surface energy are better matched.

On the other hand, the ethyltriglycol coating did not seem to affect the surface energy of the acid-etched PPE significantly, only an increment of 2–4 mN/m was observed in Dyne test pen measurements. However, since the test accuracy was limited to 2 mN/m, it was hard to confirm whether the surface energy had been changed.

Table 3. Measured surface energies for each test substrate type.

Substrate	Surface energy [mNm^{-1}]
Native PPE (injection-molded)	30–32
O_2 plasma treatment	≥60
Nanoflame treatment	≥60
Ethyltriglycol coating	33–39

H_2SO_4 coating & ethyltriglycol coating	58–60
Extruded PPE	30–32

3.1.2. Surface profile

Figure 2 presents the surface profile measurement results. Plasma treatment results, which the authors obtained earlier [13], are used here as a reference for comparison with the other treatments. We observed that all of the chosen surface treatments alter the substrate surface profile. Applying chemical coating to the native PPE increased the surface roughness, and chemical coating of the acid-etched substrate led to significant alteration of the surface profile. In addition, a rather rough surface was obtained with the Nanoflame treatment, although modification was not as significant as with the plasma treatment. The results obtained from the extruded PPE are presented in a separate graph, since the roughness parameters of the extruded substrate are

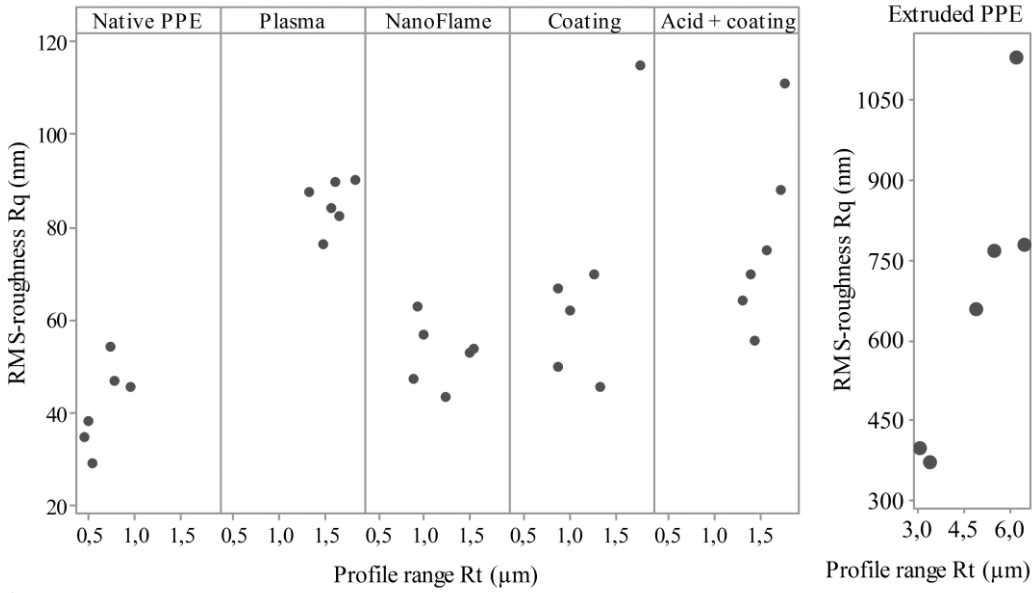

an order of magnitude higher when compared to the other results.

Figure 2. Measured surface profiles of the native, injection-molded PPE and of the substrates with surface pre-treatments. Extruded substrate results are included in a separate graph. Measured RMS roughness R_q is presented as a function of the profile range R_t.

3.2. Print quality

Figure 3 shows the measured line widths of the printed traces. A comparison was made between the traces printed with all the inks on native PPE samples and the traces printed on significantly altered substrates: plasma treated, acid etched + ethyltrigycol coated, and extruded PPE. Here, the line widths 1300 μm and 1400 μm were used as reference lines to improve the readability.

We observed differences between the inks that were used. We also observed significant spreading from the target width of 1300 μm with almost all ink-substrate combinations; best control over line width was obtained with aqueous HPS-021LV ink, whereas other inks spread significantly on similar substrates. Water surface tension (approximately 72mN/m) [39] is high compared to the measured PPE surface energy, 30–32 mN/m, and wetting was thus more controlled. According to manufacturer information, the surface tension of other solvents is similar or even lower than PPE substrate surface energy, and thus they are more likely to spread.

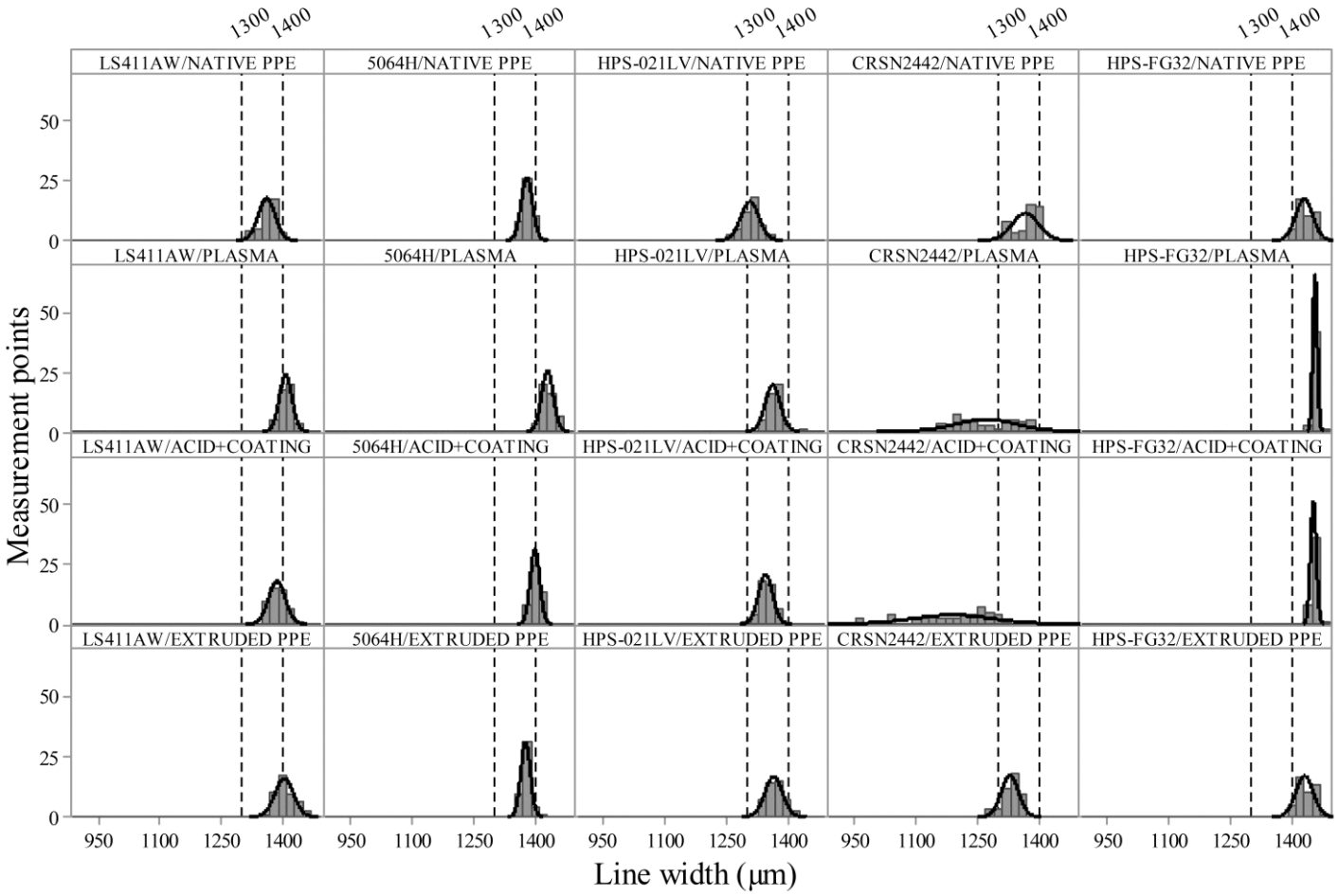

Figure 3. Measured line widths for all inks on native PPE, plasma treated PPE, acid-etched and coated PPE, and extruded PPE.

Furthermore, we noted that the substrate surface parameters affect the line spreading of the inks. The measurement data in figure 3 indicates that both increased surface energy (plasma and combined chemical treatment) and increased surface roughness (extruded PPE) enhanced line spreading compared to results measured on native PPE substrates. Since the measured lines were even 100 µm wider than the targeted values, it might be necessary to consider alternative surface modification methods whenever finer features of printed patterns are required. It has been demonstrated earlier that these pastes can be used to fabrifcate relatively fine features by screen printing: Kujala showed in [40] that both DuPont 5064H and Asahi LS411AW inks can be

used to print 50 µm wide vias, and conductive traces with line width below 500 µm. Additionally, SunChemical CRSN2442 and Novacentrix HPS-021LV inks have been succesfully used to fabricate narrow lines with screen printing [41,42]. Above-mentioned features are close to the limits of screen printing processing, even though they are still coarse in comparison to for example laser-shaped LTCC conductors [43]. However, our aim is for large area electronics, and therefore, screen printing is considered a sufficient fabrication method for our purposes.

We observed abnormally narrow lines and deviation in the measured widths in the CRSN2442 data on plasma-treated substrates and on ethyltriglycol-coated, acid-etched substrates. This behavior was most likely caused by variation in the ink volume on the screen during printing and simultaneous screen clogging. Therefore, no conclusions can be made regarding CRSN2442 ink spreading abilities on those substrates.

In addition to variations in line spreading, we noted differences in both line thickness and roughness between the inks that were used. The measured line thicknesses and conductor surface roughnesses are presented in figure 4a, where the line thickness was obtained from the measured profile range value R_t, and the conductor surface roughness was obtained from the measured RMS roughness R_q.

We obtained approximately 25% thinner lines with the HPS-FG32 than with other inks. On the other hand, this ink tended to spread more. Significant deviation in the measured thickness data of the HPS-021LV and Asahi LS411AW inks was observed. All of the inks were printed using the same screen, and it is likely that the parameters of those inks caused the variations. Asahi LS411AW viscosity is significantly higher than the viscosities of other inks (table 1), which may have a negative effect on process control. In contrast, HPS-021LV viscosity is the lowest of the used inks (table 1), and the ink tends to try rapidly during printing due to water evaporation. Therefore, the ink volume is harder to control.

We observed differences between the used inks in the roughness data. Normalized surface roughness by line thickness is presented in figure 4b. The line roughness of HPS-FG32 can be partially explained by flake composition: the SEM image (figure 5b) indicates that ink flakes form a rather loose structure,

increasing surface roughness. On the other hand, the formed lines are widely spread and thin, which may have a negative effect on the surface roughness.

On the contrary, LS411AW flake size varied (figure 5c), thus enabling a relatively smooth conductor surface compared to the obtained thickness values. Furthermore, comparison of the HPS021LV roughness data (figure 4b) and flake composition (figure 5e) indicates that the compact flake structure of cured ink enables a relatively smooth conductor surface. The lowest relative roughness was obtained with 5064H ink, with the conductor surfaces being rather smooth compared to the other inks, even though more variation in the results could be observed.

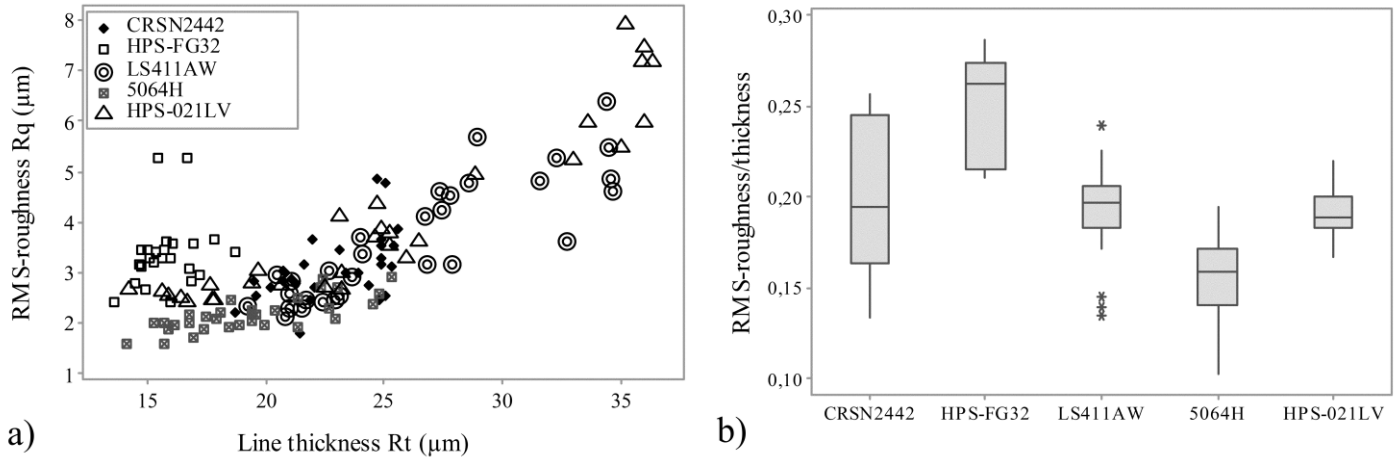

Figure 4. a) Measured conductor RMS roughness R_q as a function of measured conductor line thickness R_t with the used silver inks; b) RMS roughness R_q, normalized by measured conductor line thickness R_t.

We observed significant variation in CRSN2442 line roughness in relation to the obtained thickness, with the mean value being close to the overall average roughness obtained with the used inks. The cured structure appears to consist of spherical particles and flakes (figure 5a), and variations in the roughness were most likely related to printing parameters, such as screen pressure. It is also possible that ink rheology affected the results. In total, measured roughness values are rather convenient, considering that the particle size of these inks is on the micrometer scale, and particles are overlapping in the cured structure.

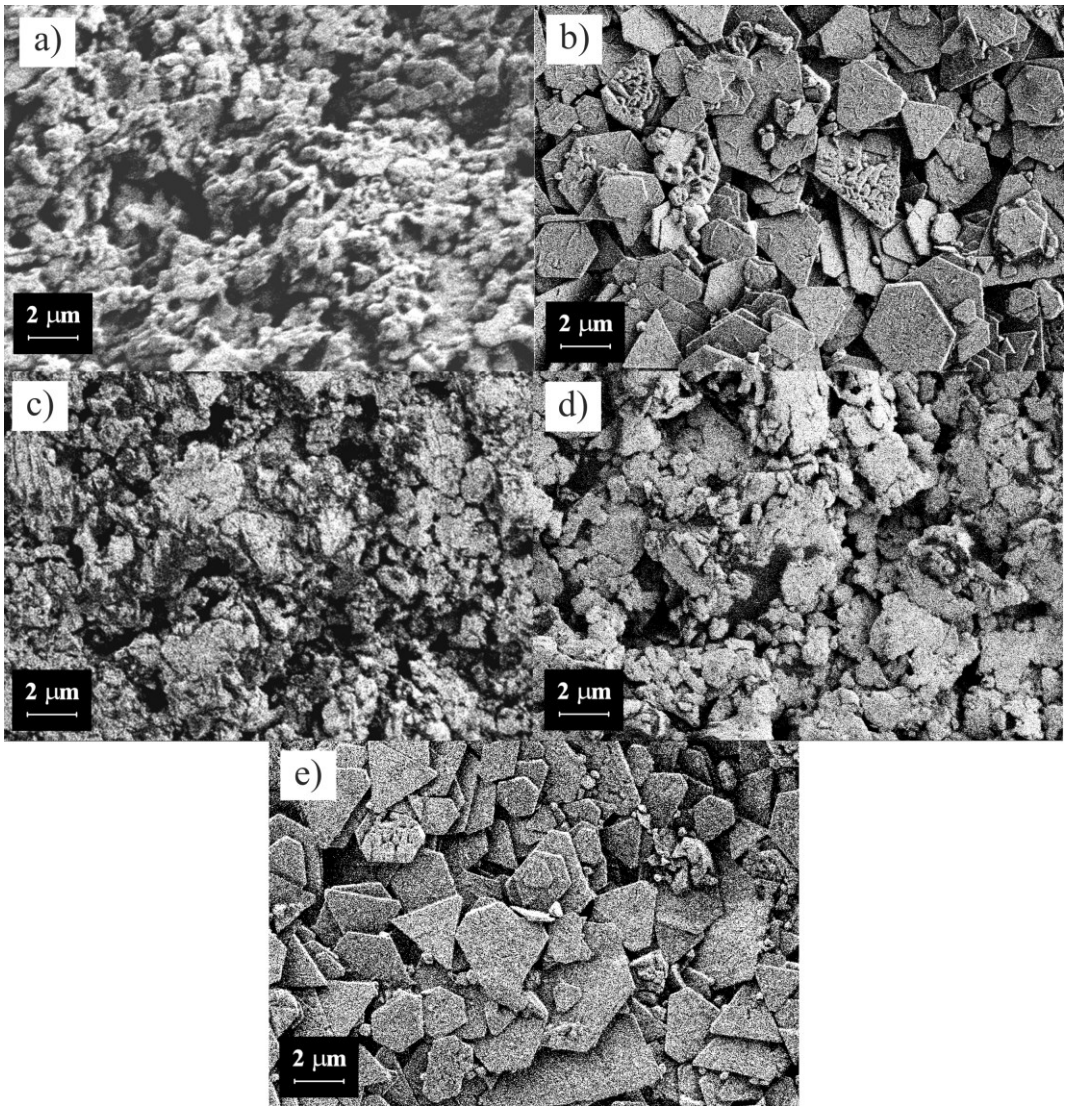

Figure 5. SEM images of the conductor surface of a) CRSN2442 ink, b) HPS-FG32 ink, c) LS411AW ink, d) 5064H ink, and e) HPS-021LV ink. Magnification 15k, EHT voltage 1.00 kV.

3.3. Electrical performance

Sheet resistances calculated by (3) from the measured currents and voltages are presented in figure 6. In figure 6, 10 mΩ/□ and 20 mΩ/□ are used as reference lines, since the lowest measured values were approximately 10 mΩ/□ and a sheet resistance of 20 mΩ/□ was still sufficient, when considering future research.

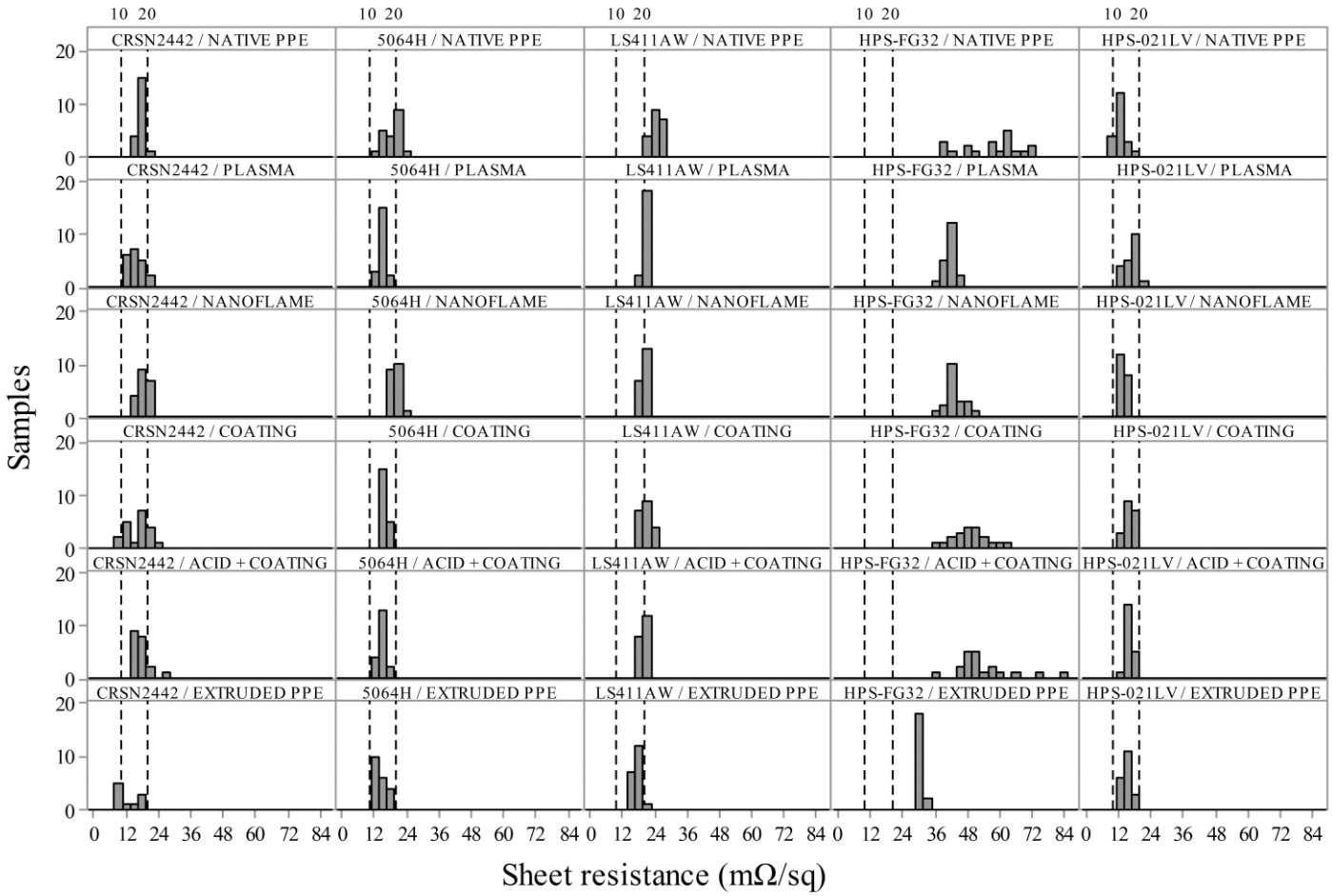

Figure 6. Measured sheet resistances with each ink/substrate combination.

The measured HPS-FG32 sheet resistances were more than two times higher than the measured values of the other inks, indicating poor conductivity. After analyzing the first sample set, we fabricated new HPS-FG32 samples on a few selected test substrates with doubled curing time. These experiments were conducted in order to investigate the effect of curing conditions on sheet resistance. The test parameter and result summary are given in table 4. We observed that a longer curing time provided better electrical performance, but the sheet resistance values were still high in comparison to other inks. Even though narrow lines with higher thickness could be produced, resistance would still be high, according to manufacturer information. Therefore, it may be concluded that this material is not competitive with other inks.

Table 4. Measured HPS-FG32 sheet resistances with different curing conditions.

Substrate	Sheet resistance: Curing 140 °C/10 min	Sheet resistance: Curing 140 °C/20 min
Native PPE	56.53 ± 11.08 mΩ/□	43.54 ± 2.52 mΩ/□
O_2 plasma treated PPE	41.31 ± 2.21 mΩ/□	40.63 ± 1.62 mΩ/□
acid etched and coated PPE	53.47 ± 11.11 mΩ/□	54.95 ± 5.52 mΩ/□

Comparison of other inks indicated that the lowest sheet resistances, between 10–20 mΩ/□, are obtained with HPS-021LV, 5064H, and CRSN2442, whereas LS411AW sheet resistances are a little higher, approximately 15–25 mΩ/□. However, these values are still sufficient for our purposes. In general, the obtained sheet resistance values match the datasheet information when the measured line thickness values are considered. However, we did observe significant deviation in the measured values. To improve sheet resistance stability, decreasing variation in both the line thickness and roughness through better process control would be necessary. In addition, better control over variations in line spreading would be required.

Furthermore, process optimization would provide benefits at high frequencies. Even though the measured sheet resistances are suitable for HF applications, as stated earlier by, for example, Halonen [32], it has been observed [7,32,44] that many other parameters, such as substrate surface and conductor roughness, affect HF performance greatly. Therefore, process optimization is required in order to produce high-quality HF conductors. For example, the current density is packed to the conductor surface due to the skin effect at high frequencies, and thus a rough conductor surface lengthens the signal path, increasing signal losses [7,44,45].

3.4. Mechanical performance

3.4.1. Adhesion after curing

The results of the ASTM-D3359 crosscut adhesion test are presented in figure 7. A few samples had to be discarded from the analysis since ink adhesion failed due to imperfections in the substrate surface caused by

the injection-molding process. Therefore, those results are not comparable to results obtained on a smooth

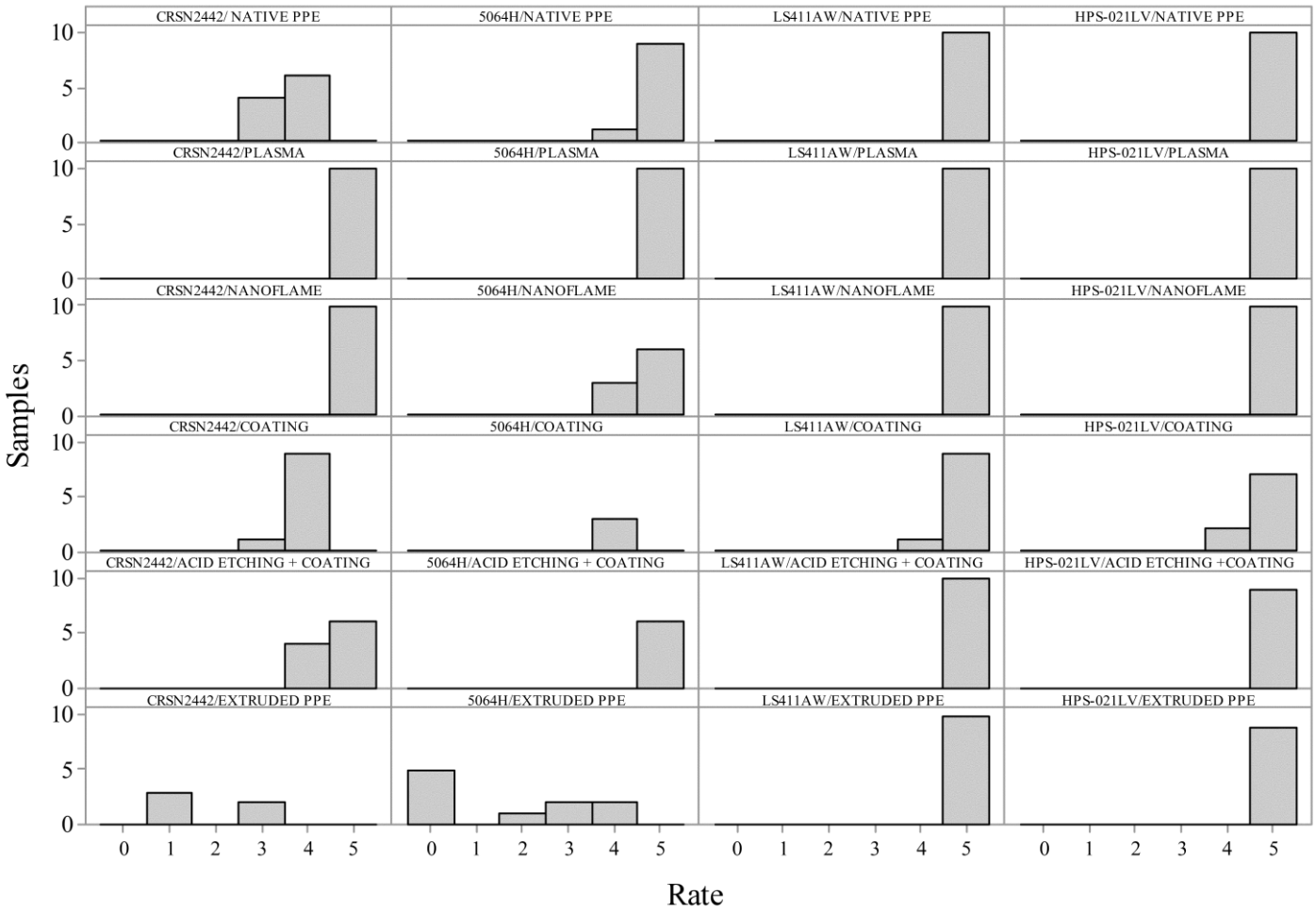

substrate surface.

Figure 7. ASTM-D3359 test results for each ink/substrate combination.

These results indicate that the adhesion of LS411AW, 5064H, and HPS-021LV inks was excellent, even on the native PPE substrates. On the other hand, as observed already in [13], CRSN2442 adhesion was poorer (ink removal 5–15%) on the native PPE substrates. However, the surface treatments that were used seem to have improved the adhesion of this ink, and ink removal could be reduced to 0–5%. Therefore, it is likely that new functional groups have been formed on PPE surface, enhancing ink adhesion. Furthermore,

effect on adhesion has been most significant with those treatments that caused both increment in surface energy and in surface roughness.

On the other hand, chemical coating on native PPE had no effect on ink adhesion. Even though ink removal seems to have increased with few inks using this treatment, more experiments would be needed to confirm if this treatment has any effect on adhesion level. It is also possible that poor wetting on native PPE prevents this chemical from adhering well to substrate, and thus, this coating layer might be removed with ink in the crosscut test. Additionally, it should be noted that since chemical coating was first cured at 100 °C, and inks printed on top of this coating were annealed at higher temperatures, it is possible that interaction of chemical coating with printed pastes is excessively enhanced. Therefore, it would be beneficial to determine, whether different results would be obtained using ink annealing temperatures not exceeding chemical curing temperature.

In addition, we observed that printing on the extruded substrate led to significant variation in the adhesion level. LS411AW and HPS-021LV adhesion was excellent even on this substrate, whereas significant adhesion failures were observed with the 5064H and CRSN2442 inks. This difference was most likely caused by the extremely rough surface, which prevented the interlocking of the latter inks. These results emphasize the importance of balance between the substrate surface chemistry and roughness: surface roughness may have a positive effect on ink bonding on a hydrophilic substrate, but a rough surface of a hydrophobic compound may weaken the bonds between the ink and substrate, consequently weakening the adhesion [46].

The HPS-FG32 results were not included in this analysis, since we noted that the first sample batch of HPS-FG32 ink had not dried properly: ink cohesion of all the samples failed in the crosscut test. Further inspection revealed that the remaining ink layer on the substrate was conductive, whereas the removed ink layer was not. Furthermore, since the sheet resistance of the second batch was still insufficient for further research, the ink was discarded from further analysis, and thus ink adhesion was not evaluated.

3.4.2. Effect of environmental stress

Based on both the sheet resistance measurements and the initial adhesion evaluation, we chose the best material combinations for the environmental reliability tests. Since both the electrical and mechanical performance of the LS411AW, 5064H, and HPS-021LV inks were excellent, they were selected for further experiments. We selected an oxygen plasma treatment and the combined treatment of acid etching and chemical coating as substrate treatment methods. These treatments had the most significant effect on surface roughness and energy, and their effect on ink adhesion was positive. A native, injection-molded PPE was used as a reference substrate for evaluating these pre-treated substrates. The fabricated sample sets are presented in table 5.

Figure 8 shows the effects of environmental stress on the ink-substrate interface behavior. Further discussion of different failure types is provided as supplementary information. Adhesion of the samples remained excellent in high relative humidity and elevated temperature of the 85 % RH/85 °C test, since the adhesion of only three samples printed with DuPont 5064H ink failed, and therefore, no degradation of the adhesion level could be observed. These results are in line with work done by Putaala et al. [3], where RFID tags printed on different polymer compounds and reliability in the 85 % RH/85 °C test was evaluated. Their samples did not fail until over 1000 h exposure to these conditions.

Table 5. Fabricated sample sets for reliability tests with chosen inks and substrates.

Set	Ink	Substrate	85 % RH/85 °C	Salt mist
1	LS-411AW	Native PPE	x	x
2	LS-411AW	Plasma treated	x	x
3	LS-411AW	Acid etched & coated	x	x
4	5064H	Native PPE	x	x
5	5064H	Plasma treated	x	x
6	5064H	Acid etched & coated	x	x
7	HPS-021LV	Native PPE	x	x
8	HPS-021LV	Plasma treated	x	x
9	HPS-021LV	Acid etched & coated	x	x

We observed several cohesion failures with HPS-021LV ink. The removed ink layer was extremely thin, indicating that moisture had penetrated the outer surface of the samples during the test, but that the corrosive effect was not severe. Additionally, the substrate cohesion of a few samples failed, indicating that the PPE-based compound was affected by the test conditions. The least number of failures occurred with the native PPE samples, where a 0–5% failure rate was observed.

On the other hand, more substrate failures occurred with the surface pre-treated samples, where we observed substrate cohesion failures even in 20% of the samples. Therefore, it is possible that these surface pretreatments decrease the moisture resistance of the PPE compound. Still, these results are promising considering the fact that common PE substrate materials, such as polyimide (PI) and polyethylene terephtalate (PET), typically have severe issues related to moisture absorbance, and are thus susceptible to environmental stress [47,48].

In contrast to results from the 85 % RH/85 °C test, exposure to NaCl mist in a humid environment lowered the adhesion level significantly. In addition to adhesion failures, a significant number of ink cohesion failures occurred with all inks, and substrate surface cohesion failed as well.

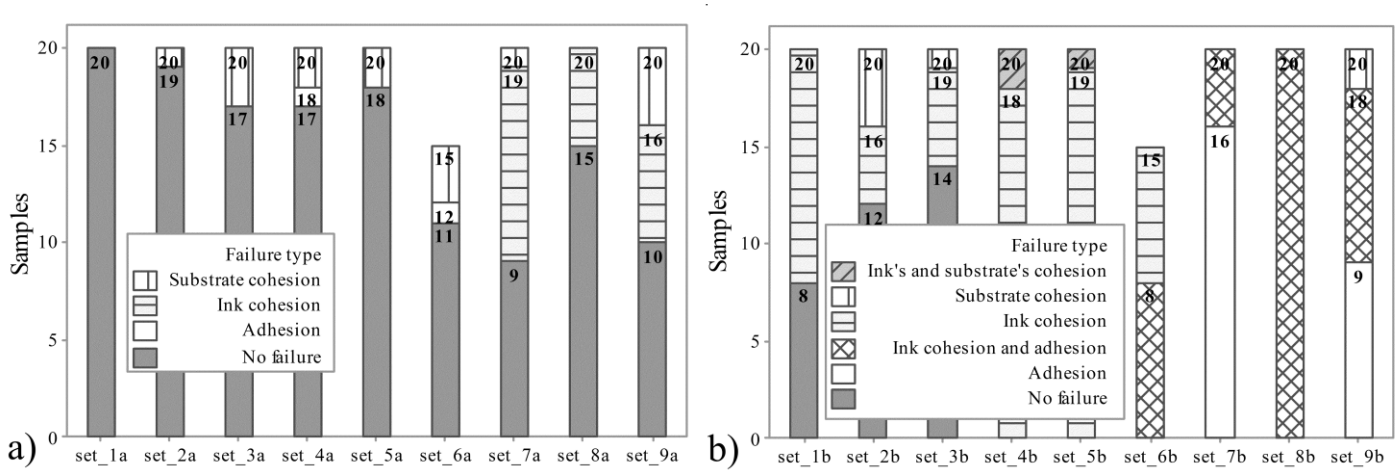

Figure 8. Ink-substrate interface: adhesion and cohesion failures after a) 85 % RH/85 °C test and b) salt mist test. Sets 1–3 were printed with Asahi LS411AW ink, sets 4–6 were printed with DuPont 5064H ink, and sets 7–9 were printed with Novacentrix HPS-021LV ink. Sets 1, 4, and 7 were printed on a

native PPE substrate, sets 2, 5, and 8 on a plasma treated PPE substrate, and sets 3, 6, and 9 on an acid-etched and chemically-coated PPE substrate.

After conducting the salt mist test, we observed areas with color alterations in the silver surface of the samples fabricated with LS411AW and 5064H inks. The 5064H alteration was more significant and its effect on ink cohesion was more severe. The SEM images obtained from our samples with dark areas indicate that new crystal particles formed on top of the silver layer. These results are presented in figure 9. Prior studies have found that in highly humid conditions, silver tends to react with NaCl, creating silver chloride (AgCl) crystals on a silver surface [49–51]. Therefore, it is possible that the crystal particles observed in this study consisted of AgCl. On the other hand, it has been observed that in a salt spray chamber, it is possible that the AgCl that forms dissolves in NaCl, and that new, big Ag particles may form [49–51]. Additionally, other corrosion products, such as oxides and other chlorides, have been observed. In our study, the size of the detected particles varies from tens of nanometers to several micrometers, suggesting that several corrosion products may have formed on the samples.

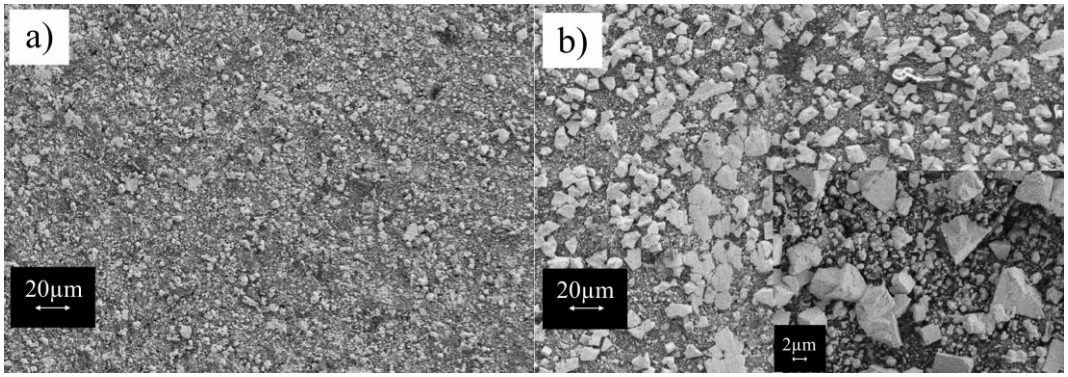

Figure 9. SEM images obtained from a) the middle of the 5064H ink surface b) the edge of the 5064H ink surface. Magnification 917; EHT voltage 3.00 kV.

We also observed that these particles had formed particularly at the edges of the silver-coated area, whereas the center of the samples was not significantly corroded. Since we also observed that the flake

structure is more compact in the middle of the samples, it can be concluded that reactions causing silver surface darkening could not take place in the middle due to the surface composition. It is also possible that the printing process made the sample edges rougher.

During the crosscut test, we observed that only the thin, darkened silver layer was removed from the top of the LS411AW and 5064H samples, whereas the rest of the silver coating remained intact, indicating that corrosive reactions affected only the surface area of the silver layer. However, we could not classify the adhesion of these samples since cohesion failures have not been included in the ASTM-D3359 standard.

In contrast, we could not observe visual alterations in the HPS-021LV samples. This difference was most likely caused by the flake topologies (figure 5e): HPS-021LV flakes seem to form a more compact structure than other ink flakes, possibly because there are less solvent residues left after curing in low temperatures, since the water boiling point is reached below those temperatures. Therefore, the sprayed NaCl cannot interact with printed silver that easily. It is also possible that the corrosion products later dissolved into the NaCl solution in the salt spray chamber, but Ag corrosion still took place [49].

The classification results for the remaining samples without cohesion failures are presented in figure 10 for the 85 % RH/85 °C test and the salt mist test, respectively. Since the 85 % RH/85 °C test did not affect the ink-substrate interface properties, adhesion remained excellent. LS411AW survived both tests extremely well, even the salt mist test did not degrade its adhesion on any substrate. In addition, 5064H adhesion degradation was not significant, since ink removal was still 5% or less, even after the salt mist test.

In contrast, HPS-021LV adhesion degraded even from 0% ink removal to more than 65% removal after the salt mist test. Additionally, we observed both ink cohesion and adhesion failures in several samples, and no samples survived this test without any failures. Therefore, it may be concluded that this test was extremely severe for this ink type, even though no visual signs of corrosion could be observed. Therefore, it is possible that even though HPS-021LV composition after curing seems more compact than the composition of other inks, residues of the solvents and binders in other inks provide better protection against environmental corrosion.

Additionally, we noted that the effect of the substrate surface pre-treatment on adhesion was significant in this test, since ink removal on acid-etched and coated samples was only 5%, compared to 65% removal on native PPE. Adhesion on plasma-treated samples also seemed to remain tolerable, but since ink cohesion failed on all samples, the adhesion could not be classified. This result indicates that strong chemical bonds are necessary for reliable printed structures, and it likewise suggests that organic components would be beneficial for this ink composition, too.

Again, an effect on the substrate cohesion after exposure to environmental stress was observed, with a failure rate of 5–20% occurring in several sample sets. Even though the exposure time in this test was rather short compared to the 85 % RH/85 °C test, we still observed almost as many substrate failures. These results emphasize the harshness of this kind of environment. However, as concluded in, for example [49–51], in a standard salt chamber environment there are less reactive species, like sulfides or ozone, in the air, and therefore, the corrosion in a salt chamber is negligible in comparison to a real marine environment. Therefore, intense protection of the printed structures is required in marine applications.

Here, we observed that environmental stress can cause cause drastic adhesion degradation of printed silver on a polymer substrate. These findings are similar to those of Xie, Caglar and Halonen [2, 31, 32]. As mentioned earlier, we did not measure in-situ sheet resistance of the samples during the reliability tests or the sheet resistance after reliability tests, because it has been stated before for example in [2, 31, 32] that effect on silver resistance is not significant even after the salt fog test, even though resistance increment up to 6-21% may occur. However, this change is negligible in comparison to the observed adhesion degradation. Additionally, severe demalination of conductive traces eventually leads to system failure, independent on electrical performance. Therefore, electrical performance optimization will be beneficial only after adhesion issues have first been solved, as emphasized in [32], where a protective layer was applied, and no change in sheet resistance occurred in any conditions. Still, adhesion degradation was significant, even though similar protective coating was used. Of course, maintaining sufficient conductivity level is important, and in further stages, it would be beneficial to confirm electrical performance after exposure to environmental stress, and to

investigate both the possible effect of protective coatings, and the impact of environmental stress on HF performance [32]. Sheet resistance determination can be made both in situ and consequently, as demonstrated for example in [43].

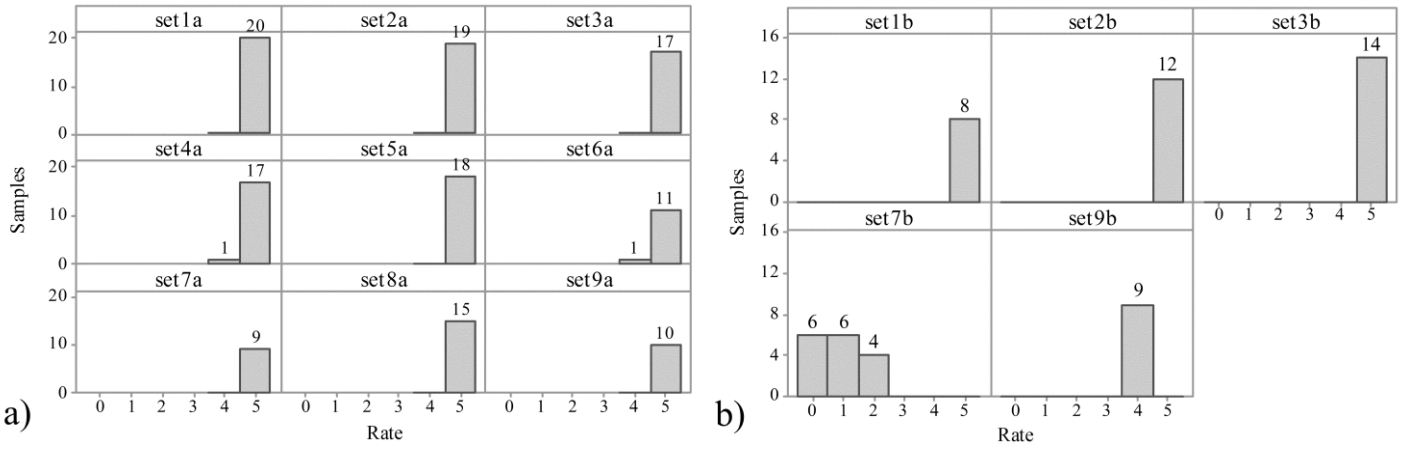

Figure 10. Ink-substrate interface: adhesion and cohesion failures after a) 85 % RH/85 °C test and b) salt mist test. Sets 1–3 were printed with Asahi LS411AW ink, sets 4–6 were printed with DuPont 5064H ink, and sets 7–9 were printed with Novacentrix HPS-021LV ink. Sets 1, 4, and 7 were printed on a native PPE substrate, sets 2, 5, and 8 on a plasma-treated PPE substrate, and sets 3, 6, and 9 on an acid-etched and chemically-coated PPE substrate.

3.5. Discussion

A comparison of the line widths measured with an optical microscope revealed that surface treatments tend to increase the conductor line width. Based on these results, it may be concluded that both increased surface energy and a roughened substrate surface clearly promote ink spreading on this low-surface energy substrate.

In addition, we found differences between the inks that were used. Inks with organic solvents resulted in wider lines than originally designed, whereas the spreading of lines printed with aqueous HPS-021LV was more controlled.

Significant line spreading is often problematic in such applications, where the downscaling of printed features is necessary. Additionally, in some other application consider areas, narrower structures would be crucial and

alternative methods should be considered. However, the aim of our work was to find solutions for such antennas and base station structures, where the miniaturizing of electronics is not essentially required. Therefore, wide lines and line spreading are not a significant issue for future work, especially when taken into account in feature design.

Several of the inks chosen seem suitable for HF applications based on the obtained low sheet resistance values. Still, further investigation is required in order to confirm the effects of conductor surface roughness on the final performance.

In addition, we observed that the surface treatments that were used could improve adhesion significantly. In particular, the Nanoflame treatment and chemical coating on the acid-etched substrate improved the results and ink removal was reduced to 0%, even when the removal was originally 15%. The authors also observed that the oxygen plasma treatment had a similar promoting effect on adhesion, which is in line with previous findings [13]. These results indicate that both an increment of surface energy and surface roughening are needed to promote ink adhesion on this substrate material.

In addition to the initial adhesion strength, the surface treatments had a positive effect on the sample reliability. However, as observed after the salt mist test, sufficient protection of the printed structures is necessary in harsh conditions to prevent both adhesion and cohesion failures in the used materials. Second, such protection would help maintain electrical performance at the required level.

The significance of the ink composition in regards to reliability was emphasized in these tests. Furthermore, the results indicate that surface pre-treatments might damage the substrate by, for example, increasing moisture absorption. Additionally, the possible effects of the surface treatments on high frequency characteristics of the used PPE substrate are still unknown, and they require further investigation before these treatments can be utilized in printed HF applications on this substrate.

4. Conclusion

In this study, we studied the performance of five commercially available silver inks on a PPE-based substrate. We inspected the effect of surface pre-treatments on test substrates by analyzing both the surface properties and final performance of the printed structures. In addition, we used environmental stress tests to evaluate the long-term reliability of the printed structures.

The results indicate that such commercial inks are able to provide both low sheet resistance and excellent adhesion on the test substrates. On the other hand, by choosing a suitable surface treatment, the substrate-ink interface performance may be improved significantly, and thus the variety of suitable inks may be widened.

The environmental reliability test results indicate that the test structures were able to withstand even rather harsh conditions. However, in extremely harsh conditions, such as a marine environment, it is important to provide sufficient environmental protection, such as barrier layers, to ensure the long-term reliability of applications.

Our results indicate that PPE is a sufficient substrate material for large area printed electronics. In this study, we concluded that both the materials and process parameters affect the final print quality, and thus, also the conductor performance. Therefore, further research is needed to optimize both the material parameters and fabrication process. Other recommendations for future work include HF characterization for both the test substrates and inks. In addition, protection methods against environmental stress should be studied.

Acknowledgements

R.M. designed and performed the experiments related to substrate surface analysis and characterization of the printed structures. In addition, R.M. analyzed the measurement data. M.M. supervised the research and participated in experiment design and data analysis. The manuscript and figures were prepared by R.M. Both authors reviewed the manuscript.

This work was supported by the Finnish Funding Agency for Technology and Innovation (Tekes) [grant number 2742/31/2016.] M.M. is supported by the Academy of Finland [grant numbers 288945 and 294119]. We greatly thank Juha Pippola and Janne Kiilunen for their contributions to the design and performance of the environmental stress tests. In addition, we would like to thank the Premix company for providing the test substrates.

References

[1] H. Sillanpää, Ph.D. Thesis, Tampere University of Technology, June, 2014.

[2] L. Xie, M. Mäntysalo, A. L. Cabezas, Y. Feng, F. Jonsson, L. Zheng, Electrical performance and reliability evaluation of inkjet-printed Ag interconnections on paper substrates, Mater. Lett. 88(2012) 68–72. https://doi.org/10.1016/j.matlet.2012.08.030.

[3] J. Putaala, J. Niittynen, J. Hannu, S. Myllymäki, E. Kunnari, M. Mäntysalo, J. Hagberg, Capability assessment of inkjet printing for reliable RFID applications, IEEE Trans. Device Mater. Reliab., 17(2017) 281–290. https://doi.org/10.1109/TDMR.2016.2636342.

[4] Y. S. Rim, S-H. Bae, H. Chen, N. De Marco, Y. Yang, Recent Progress in Materials and Devices toward Printable and Flexible Sensors, Adv. Mat. 28(2016) 4415–4440. https://doi.org/10.1002/adma.201505118.

[5] Z. Bao, X. Chen, Flexible and Stretchable Devices, Adv. Mat. 28(2016) 4177–4179. https://doi.org/10.1002/adma.201601422.

[6] S. Khan, L. Lorenzelli, R. S. Dahlya, Technologies for Printing Sensors and Electronics Over Large Flexible Substrates: A Review, IEEE Sens. J., 15(2015) 3164–3185. https://doi.org/10.1109/JSEN.2014.2375203.

[7] N. Komoda, M. Nogi, K. Suganuma, K. Kohno, Y. Akiyama, K. Otsuka, Printed silver nanowire antennas with low signal loss at high-frequency radio, Nanoscale, 4(2012) 3148–3153. https://doi.org/ 10.1039/C2NR30485F.

[8] A. B. Menicanin, L. D. Zivanov, M. S. Damnjanovic, A. M. Maric, Low-Cost CPW Meander Inductors Utilizing Ink-Jet Printing on Flexible Substrate for High-Frequency Applications, IEEE Trans. Electron Devices, 60(2013) 827–832. https://doi.org/ 10.1109/TED.2012.2234461.

[9] U. Zorll, in: A.A. Tracton (Ed.), Coatings Technology: Fundamentals, Testing and processing techniques. CRC Press, 2006, Ch. 6.

[10] P. De Gennes, F. Brochard-Wyart, D. Quéré, Capillarity and Wetting Phenomena; Drops, Bubbles, Pearls, Waves, Springer Science and Business Media, Inc., NY, USA 2004.

[11] R. K. Ulrich, in: R. K. Ulrich, W.D. Brown (Eds.), Advanced Electronic Packaging, Wiley, 2006, pp. 651–690.

[12] J. Lilja, V. Pynttäri, T. Kaija, R. Mäkinen, E. Halonen, H. Sillanpää, J. Heikkinen, M. Mäntysalo, P. Salonen, P. De Maagt, Body-Worn Antennas Making a Splash: Lifejacket-Integrated Antennas for Global Search and Rescue Satellite System, IEEE Trans. Antennas Propag., 55(2013) 324–341. https://doi.org/10.1109/MAP.2013.6529385.

[13] R. Mikkonen, M. Mäntysalo, Benchmark study of screen printable silver inks on a PPE based substrate, in Proc. of 21st EMPC 2017, Warsaw, Poland, 11th–13th September, 2017. In press.

[14] Preperm®L260, TDS, Premix Oy.

[15] E. Sipilä, J. Virkki, L. Sydänheimo, L. Ukkonen, Experimental Study on Brush-Painted Passive RFID-Based Humidity Sensors Embedded into Plywood Structures, International Journal of Antennas and Propagation, 2016(2016). http://dx.doi.org/10.1155/2016/1203673.

[16] T. Björninen, J. Virkki, L. Sydänheimo, L. Ukkonen, Manufacturing of antennas for passive UHF RFID tags by direct write dispensing of copper and silver inks on textiles, *Proc. of ICEAA 2015*, IEEE. (2015) 589–592. https://doi.org/10.1109/ICEAA.2015.7297183.

[17] T. Happonen, T. Ritvonen, P. Korhonen, J. Häkkinen, T. Fabritius, Bending reliability of printed conductors deposited on plastic foil with various silver pastes, The International Journal of Advanced Manufacturing Technology, 82(2016) 1633–1673. https://doi.org/10.1007/s00170-015-7403-9.

[18] E. Jansson, J. Hast, J. Petäjä, J. Honkala, J. Häkkinen, O. Huttunen, Improving Conductivity of Rotary Screen Printed Microparticle Silver Conductors Using a Roll-to-Roll Calendering Process, Journal of Print and Media Technology Research, 4(2015) 19–26. https://doi.org/10.14622/JPMTR-1442.

[19] J. V. Voutilainen, T. Happonen, J. Häkkinen, Reliability of silkscreen printed planar capacitors and inductors under accelerated thermal cycling and humidity bias life testing, Proc. of 4th ESTC, (2012) 1–6. https://doi.org/10.1109/ESTC.2012.6542201.

[20] CRSN2442 Conductive Silver Ink, TDS, SunChemical.

[21] 5064H, TDS, DuPont..

[22] Metalon HPS-FG32 silver screen ink, TDS, Novacentrix. Available: https://www.novacentrix.com/sites/default/files/pdf/Metalon%20HPS-FG32.pdf, 2016 (accessed 27 October 2017).

[23] LS411AW silver conductive paste, TDS, Asahi Chemical Research Laboratory CO., LTD.

[24] Metalon HPS-021LV silver screen ink, TDS; Novacentrix. Available: https://store.novacentrix.com/v/vspfiles/assets/images/metalon%20hps-021lv_2230.1.pdf, 2012 (accessed 27 October 2017).

[25] Polytec PT, NanoFlame Surface Pre-treatment. https://www.intertronics.co.uk/product/nanoflame-nf02-surface-pretreatment-device/, 2016 (accessed 4 April 2018).

[26] V. Pekkanen, M. Mäntysalo, K. Kaija, P. Mansikkamäki, E. Kunnari, K. Laine, J. Niittynen, S. Koskinen, E. halonen, U. Caglar, Utilizing inkjet printing to fabricate electrical interconnections in a system-in-package, Microelectron Eng., 87(2010) 2382–2390. https://doi.org/10.1016/j.mee.2010.04.013.

[27] High Modulud Polyester Monofilament Mesh for Technical Screen Printing Applications, NBC Meshtec, Inc. http://www.nbc-jp.com/eng/product/2016Alpha_l_ux_ex_spec.pdf, (accessed 4 April 2018).

[28] JEDEC Standard, JESD22-A101C Steady State Temperature Humidity Bias Life Test, JEDEC Solid State Technology Association, USA, 2009.

[29] IEC 60068 2-52, International Electrotechnical Commission, 1996.

[30] E. S. Gadelmawla, M.M. Koura, T. M. A. Maksoud, I. M. Elewa, H.H. Soliman, Roughness parameters, J. Mater. Process. technol., 123(2002) 133–145. https://doi.org/10.1016/S0924-0136(02)00060-2.

[31] U. Caglar, P. Mansikkamäki, Temperature-Dependent Reliability of Inkjet-Printed Silver Structure in Constant Humidity Environment, Proc. of NIP 24, (2008) 387–390.

[32] E. Halonen, V. Pynttäri, J. Lilja, H. Sillanpää, M. Mäntysalo, J. Heikkinen, R. Mäkinen, T. Kaija, P. Salonen, Environmental protection of Inkjet-printed Ag conductors, Mictoelectron. Eng., 88(2011) 2970–2976. https://doi.org/10.1016/j.mee.2011.04.038.

[33] ASTM-D3359-09e2, Standard Test Methods for Measuring Adhesion by Tape Test, ASTM International, USA, 2009.

[34] Y-I. Lee, Y-H. Choa, Adhesion enhancement of ink-jet printed conductive copper patterns on a flexible substrate, J. Mater. Chem., 22(2012) 12517–12522. https://doi.org/10.1039/C2JM31381B.

[35] Y. Chang, D-Y Wang, Y-L. Tai, Z-G. Yang, Preparation, characterization and reaction mechanism of a novel silver-organic conductive ink, J. Mater. Chem., 22(2012) 25296–25301. https://doi.org/10.1039/C2JM34569B.

[36] J. Park, H. Nguyen, S. Park, J. Lee, B. Kim, D. Lee, Roll-to-roll gravure printed silver patterns to guarantee printability and functionality for mass production, Current Applied Physics, 15(2015) 367–376. https://doi.org/10.1016/j.cap.2015.01.007.

[37] Y-S. Hsiao, W-T. WHang, S-C. Wu, K-R. Chuang, Chemical formation of palladium-free surface-nickelized polyimide film for flexible electronics, Thin Solid Films, 516(2008) 4258–4266. https://doi.org/10.1016/j.tsf.2007.12.166.

[38] T. Zhang, E. Asher, J. Young, A New Printed Electronics Approach Eliminating Redundant Fabrication Process of Vertical Interconnect Accesses: Building Multilayered Circuits in Porous Materials, Adv. Funct. Mater., 2018. https://doi.org/10.1002/admt.201700346.

[39] J. Kalová, R. Mareš, Reference Values of Surface Tension of Water, Int. J. Thermophys, 36(2015) 1396–1404. https://doi.org/10.1007/s10765-015-1907-2.

[40] M. Kujala. M.Sc. Thesis, Tampere University of Technology, April 2018.

[41] P. Escobedo, M. A. Carvajal, L. F. Capitán-Vallvey, J. Fernández-Salmerón, A. Martínez-Olmos, A. J. Palma, Passive UHF RFID Tag for Multispectral Assessment, Sensors, 16(2016). https://doi.org/10.3390/s16071085.

[42] W. Zhou, F. A. List, C. E. Duty, S. Babu, Fabrication of conductive paths on a fused deposition modeling substrate using inkjet deposition, Rapid Prototyping Journal, 22(2016), 77-86. https://doi.org/10.1108/RPJ-05-2014-0070.

[43] D. Nowak, A. Dziedzic, Reliability of Fine-Line Thick-Film and LTCC Conductors at High-Temperature Operation, Proc. 37th Int. Spring Seminar on Electronics Technology, ISSE (2014), 176-179.

[44] T. Björninen, S. Merilampi, L. Ukkonen, L. Sydänheimo, P. Ruuskanen, The Effect of Fabrication Method on Passive UHF RFID Tag Performance, International Journal of Antennas and Propagation, 2009(2009). http://dx.doi.org/10.1155/2009/920947.

[45] H. Yang, in: K.W. Chen (Ed.) The Electrical Engineering Handbook, Academic Press, 2004, p. 518.

[46] P. De Gennes, F. Brochard-Wyart, D. Quéré, Capillarity and Wetting Phenomena: Drops, Bubbles, Pearls, Waves, Springer Science and Business Media, Inc., New York, USA, 2004, pp. 221.

[47] S. Lahokallio, K. Saarinen, L. Frisk, Effect of High-Humidity Testing on Material Parameters of Flexible Printed Circuit Board Materials, J. Electron. Mater., 42(2013) 2822–2834. https://doi.org/10.1007/s11664-013-2652-6.

[48] B-H. Bae, M-S. Yeong, B. R. Lee, J-H. Choo, E-K. Choi, J-S. Yoon, J-B. Park, Effects of various environmental conditions on the electrical properties and interfacial reliability of printed Ag / polyimide system, Proc. of IEE. Electron. Compon. Technol. Conf. (ECTC) 64th, (2014) 1735–1739. https://doi.org/ 10.1109/ECTC.2014.6897531.

[49] H. Lin, G. S. Frankel, W. H. Abbott, Analysis of Ag corrosion products, J. Electrochem. Soc., 160(2013) C345–C355. https://doi.org/ 10.1149/2.055308jes.

[50] D. Liang, H. C. Allen, G. S. Frankel, Z. Y. Chen, R. G. Kelly, Y. Wu, B. E. Wyslouzil, Effects of Sodium Chloride Particles, Ozone, UV, and Relative Humidity on Atmospheric Corrosion of Silver, J. Electrochem. Soc., 157(2010) C146–C156. https://doi.org/10.1149/1.3310812.

[51] Y. Yoon, J. D. Angel, D. C. Hansen, Atmospheric Corrosion of Silver in Outdoor Environments and Modified Accelerated Corrosion Chambers, CORROSION, 72(2016) 1424-1432. https://doi.org/10.5006/2079.